

# Low Noise Readout using Active Reset for CMOS APS

Boyd Fowler, Michael D. Godfrey, Janusz Balicki, and John Canfield

Pixel Devices International Inc.

## ABSTRACT

Pixel reset noise sets the fundamental detection limit on photodiode based CMOS image sensors. Reset noise in standard active pixel sensor (APS) is well understood<sup>1-3</sup> and is of order  $\frac{kT}{C}$ . In this paper we present a new technique for resetting photodiodes, called active reset, which reduces reset noise without adding lag. Active reset can be applied to standard APS.<sup>4</sup> Active reset uses bandlimiting and capacitive feedback to reduce reset noise. This paper discusses the operation of an active reset pixel, and presents an analysis of lag and noise. Measured results from a 6 transistor per pixel 0.35 $\mu$ m CMOS implementation are presented. Measured results show that reset noise can be reduced to less than  $\frac{kT}{18C}$  using active reset. We find that theory simulation and measured results all match closely.

**Keywords:** Read noise, CMOS image sensors, APS, Active Reset.

## 1. INTRODUCTION

Noise in CMOS image sensors is typically much larger than in CCDs. CMOS image sensors will not displace CCDs in the market until this fundamental problem is overcome. Image sensor noise can be categorized as either fixed pattern (FPN)<sup>5</sup> or temporal.<sup>2</sup> FPN can be eliminated by using pixel to pixel offset and gain correction. On the other hand, temporal noise, after it is added to the image data, cannot be removed. Therefore techniques for reducing temporal noise in CMOS image sensors must be developed.

Temporal noise in standard photodiode APS is well understood.<sup>1-3</sup> The largest temporal noise component is contributed by resetting the pixel, and is of order  $\frac{kT}{C}$ . In CCDs temporal reset noise is eliminated by using correlated double sampling (CDS).<sup>6</sup> Due to space limitations, pixel level CDS cannot be used in APS. Pain *et al.*<sup>1</sup> present a photodiode reset technique called HTS that reduces reset noise to  $\frac{kT}{2C}$  without the addition of lag. Although this is a significant reduction in reset noise more is still required for CMOS sensors to compete with CCDs.

In this paper we introduce a new technique for resetting the pixel, called active reset, that reduces reset noise without adding lag. Active reset can be directly applied to standard APS.<sup>4</sup> Active reset uses bandlimiting and capacitive feedback to reduce reset noise. This paper discusses the operation of an active reset pixel, and presents an analysis of lag and noise. We do not analyze the effect of 1/f noise, since it is typically much smaller than the thermal and shot noise effects. In addition test results from a 6 transistor per pixel 0.35 $\mu$ m CMOS implementation are also presented and compared with both theory and simulation.

The remainder of this paper is organized as follows. Section 2 describes the operation of an active reset pixel and presents analysis of lag and noise. Section 3 presents simulation results for a 6 transistor active reset pixel. Section 4 presents measured data from a 6 transistor active reset pixel fabricated in a 0.35 $\mu$ m CMOS process. Finally, in Section 5, we compare theory, simulation, and measured results and discuss future directions.

## 2. THEORY

### 2.1. Circuit Operation

The general form of an active reset APS pixel is shown in Figure 1. It consists of two independent circuits, a readout circuit and a reset circuit. The readout circuit consists of two NMOS transistors M2 and M3, and the reset circuit consists of three NMOS transistors, M1, M5 and M4\*, and an amplifier. The operation and noise characteristics of the readout circuit have been thoroughly discussed in the literature.<sup>4,3,2</sup> Our focus in this paper is the reset circuit. Reset waveforms are shown in Figure 2. Operation of the reset circuitry is as follows. Just before  $t_1$ ,  $v_{pr}$  pulses for

---

Other author information: Email: {fowler,godfrey,balicki,canfield}@pixeldes.com; Telephone: 408-616-8852; Fax: 408-616-8852

\*Most designs do not require M4, but it lowers lag and simplifies the analysis in this paper.

approximately 100ns and pulls  $v_{pd}$  to ground. Starting at  $t_1$ ,  $v_g$  rises to  $v_{dd}$  and turns on M5, and  $v_r$  rises slowly, at  $\approx 0.1V/\mu s$ , from ground to  $\max(v_r)$  at  $t_2$ . When  $v_r$  exceeds  $v_{pd}$ , the amplifier output rises and turns on M1. Then  $v_{pd}$  follows  $v_r$  until  $v_r$  stops rising and undershoots by a few tens of millivolts, at  $t_2$ , and  $v_{pd}$  overshoots  $v_r$ .  $v_{pd}$  overshoots  $v_r$  because M1 can only pull up and  $v_r$  has undershot its maximum value. After  $v_{pd}$  overshoots  $v_r$ , the output of the amplifier  $v_1$  drops and turns M1 off. Now only the overlap capacitance of M1 is used to control  $v_{pd}$ . Finally, at  $t_3$ ,  $v_g$  falls and turns off M5. This completes reset of the pixel.

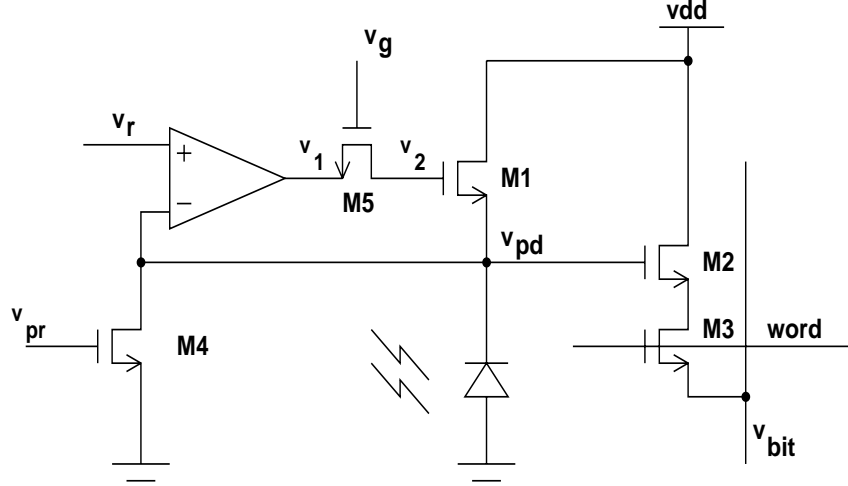


**Figure 1.** CMOS APS with Active Reset

## 2.2. Lag Analysis

Lag is defined as the amount of residual photo or dark charge left in a pixel after reset is complete. Using Figure 3, we define maximum lag as

$$\max(lag) = \left| \frac{v_{pd}(t_5) - v_{pd}(t_7)}{v_{pd}(t_4) - v_{pd}(t_7)} \right|, \quad (1)$$

where  $v_{pd}(t_5)$  is the pixel reset voltage at  $t_5$  after the maximum non-saturating input signal was collected by the pixel,  $v_{pd}(t_7)$  is the reset voltage at  $t_7$  after only dark current was collected by the pixel, and  $v_{pd}(t_4)$  is the minimum non-saturating voltage at the pixel. Assuming that M1 turns off at  $t_2^\dagger$ , we can use the small signal model in Figure 4 to estimate lag. In addition, we will assume that while  $v_g = v_{dd}$  the resistance between nodes  $v_1$  and  $v_2$  is small, i.e.  $v_1 \approx v_2$ , and  $C_l = C_{l1} + C_{l2} + 2C_{ov}$ . Equations 2 and 3 describe the small signal model, where  $g_m$  is the transconductance of the reset amplifier,  $g_o$  is the output conductance of the reset amplifier,  $C_l$  is the output capacitance of the reset amplifier,  $C_f$  is the gate to source overlap capacitance of M1,  $C_{pd}$  is the photodiode capacitance, and  $i_{pd}$  is the photodiode current.

$$(C_l + C_f) \frac{dv_1}{dt} - C_f \frac{dv_{pd}}{dt} = -g_o v_1 - g_m v_{pd} + g_m v_r \quad (2)$$

$$(C_{pd} + C_f) \frac{dv_{pd}}{dt} - C_f \frac{dv_1}{dt} = -i_{pd} \quad (3)$$

Solving equations 2 and 3, we find

$$v_{pd}(t) = k_1 e^{-t/\tau} + k_2 + k_3 t, \quad (4)$$

<sup>†</sup>This assumption is valid when the feedback loop time constant  $\tau \ll (t_3 - t_2)$ .

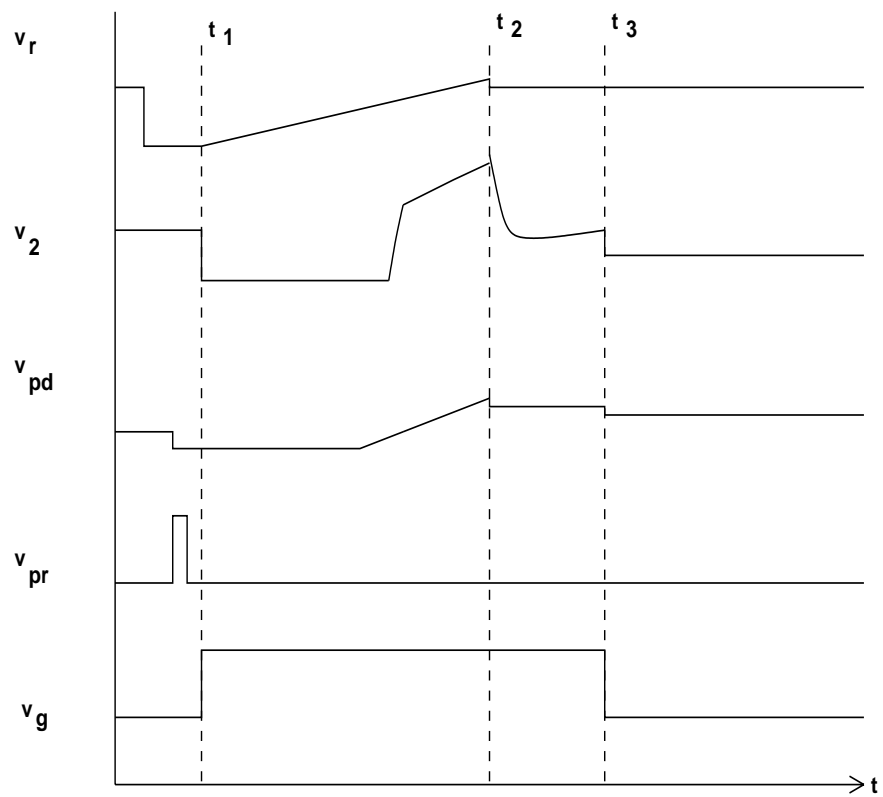


**Figure 2.** Active Reset Waveforms

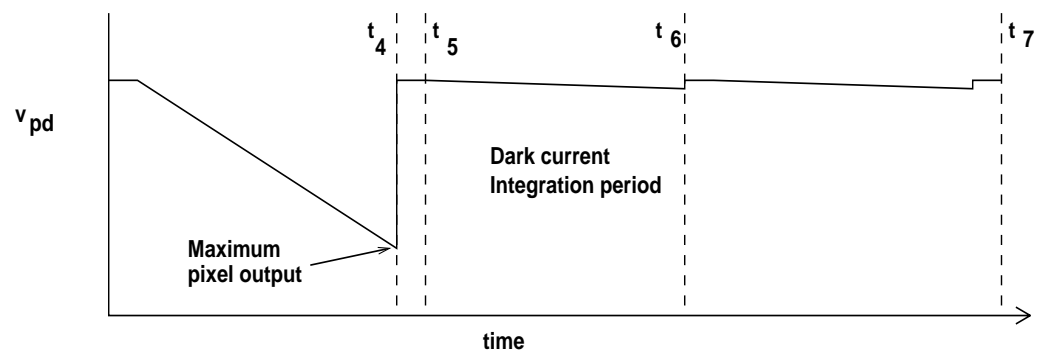


**Figure 3.** Lag Definition Waveform

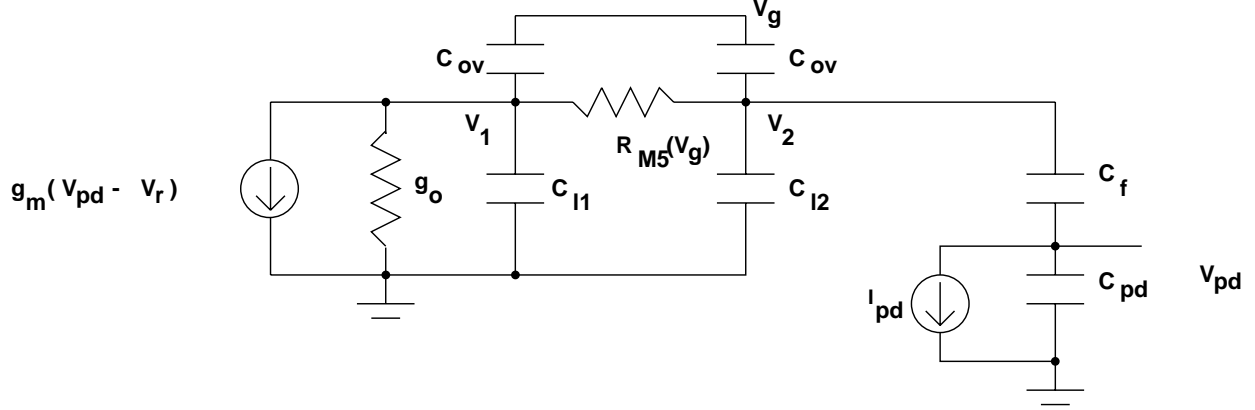


**Figure 4.** Small Signal Model of Active Reset Circuit at Time  $t_3$

$$v_1(t) = k_4 e^{-t/\tau} + k_5 + k_6 t, \quad (5)$$

where  $\tau$ ,  $k_1$ ,  $k_2$ ,  $k_3$ ,  $k_4$ ,  $k_5$ , and  $k_6$  are given in the Appendix. If we assume that  $(t_3 - t_2) \gg \tau$  then we can make the following approximations

$$v_{pd}(t) \approx k_2 + k_3 t, \quad (6)$$

and

$$v_1(t) \approx k_5 + k_6 t. \quad (7)$$

Assuming that  $v_{pd}(t_2)$  and  $v_1(t_2)$  are independent of  $i_{pd}$ , then

$$\max(lag) \approx \left| \frac{k_7 + k_8(t_3 - t_2)}{v_{pd}(t_4) - v_{pd}(t_7)} \right|, \quad (8)$$

where  $k_7$  and  $k_8$  are given in the Appendix. Using values of  $C_{pd}=25.3\text{fF}$ ,  $C_f=0.4\text{fF}$ ,  $C_l=22\text{fF}$ ,  $g_m = 2.36\mu\text{S}$ ,  $g_o = 8.3\text{nS}$ ,  $i_{pd}(t_7) = 10\text{fA}$ ,  $i_{pd}(t_5) = 2.53\text{pA}$ ,  $(t_3 - t_2) = 10\mu\text{s}$ ,  $(t_6 - t_5) = 10\text{ms}$ , and  $v_{pd}(t_4) - v_{pd}(t_7) = -1\text{V}$ ,  $\max(lag) = 0.023\%$ .

### 2.3. Reset Noise Analysis

The noise sampled onto the photodiode at  $t_3$  is the sum of the noise sampled onto the photodiode at  $t_2$  attenuated by the reset control loop, plus the noise of the reset control loop amplifier and M5.

In order to determine the reset noise we must analyze the noise sampled onto the photodiode at  $t_2$  and  $t_3$ . Noise is sampled onto the photodiode at  $t_2$  when M1 turns off. The noise sampled onto the photodiode can be determined using the small signal model in Figure 5. We again assume that while  $v_g = v_{dd}$  the resistance between nodes  $v_1$  and  $v_2$  is small, i.e.  $v_1 \approx v_2$ , and  $C_l = C_{l1} + C_{l2} + 2C_{ov}$ . To simplify analysis we introduce the following notation:  $V_{pd} = v_{pd} + V_n$ ,  $I_d = i_d + I_{dn}$ ,  $V_r = v_r + V_{rn}$ , where  $v_{pd}$  is the diode signal voltage,  $V_n$  is the diode noise voltage,  $i_d$  is the drain current in M1,  $I_{dn}$  is the noise current in  $i_d$ ,  $v_r$  is the reset voltage, and  $V_{rn}$  is the input referred reset amplifier noise voltage.  $V_{M5}$  is the thermal noise voltage of M5. We use uppercase node voltages and currents to represent random variables and lowercase node voltages and currents to represent deterministic variables. Assuming the circuit is in steady state at  $t_2$ , the noise power across the photodiode is the sum of thermal noise from the

reset amplifier, thermal noise from M5, shot noise from M1, and shot noise from the photodiode. The steady state assumption is valid when  $v_r$  rises much more slowly than the feedback loop time constant, and this is true by design for active reset. Shot noise from the photodiode and thermal noise from M5 are small and can be neglected. The input-referred two-sided power spectral density of the thermal noise in the reset amplifier is given by<sup>7</sup>

$$S_{V_{rn}}(f) = \frac{\alpha 2kT}{g_m} \quad (\text{V}^2/\text{Hz}), \quad (9)$$

where  $\alpha$  is a constant that depends on the amplifier design (it is typically between 2/3 and 2),  $k$  is Boltzmann's constant, and  $T$  is temperature in Kelvin. The two-sided power spectral density of the shot noise in M1 is given by<sup>7</sup>

$$S_{I_{dn}}(f) = qi_{pd} \quad (\text{A}^2/\text{Hz}), \quad (10)$$

where  $q$  is the charge on an electron. The noise power of  $V_n$  is given by

$$\sigma_{V_n}^2(t_2) = \int_{-\infty}^{\infty} S_{V_{rn}}(f) \left| \frac{v_{pd}}{v_r}(f) \right|^2 + S_{I_{dn}}(f) \left| \frac{v_{pd}}{i_d}(f) \right|^2 df, \quad (11)$$

where  $i_d = g_{m1}(v_2 - v_{pd}) - g_{mb1}v_{pd}$ , and  $g_{m1}$  is the gate to source transconductance of M1 and  $g_{mb1}$  is the source to body transconductance of M1.  $\frac{v_{pd}}{v_r}(f)$  and  $\frac{v_{pd}}{i_d}(f)$  are given in the Appendix.

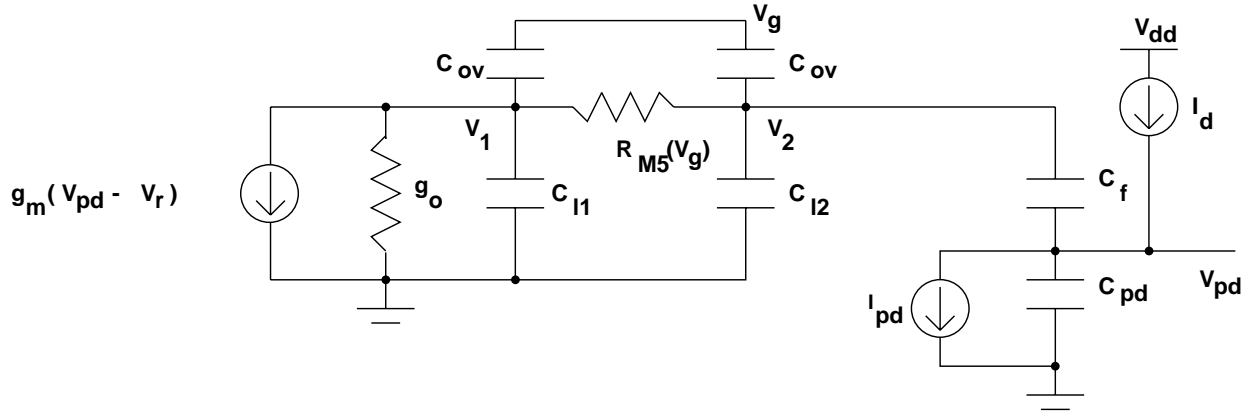


**Figure 5.** Small Signal Model of Active Reset Circuit at Time  $t_2$

Next we calculate the reset noise at  $t_3$ . Assuming that M1 turns off at  $t_2$  and the reset control loop is in steady state at time  $t_3$ , the small signal model in Figure 4 can be used for noise analysis. The steady state assumption at  $t_3$  is valid by design for active reset, i.e.  $(t_3 - t_2)$  is selected such that it is must larger than the feedback loop time constant. The total sampled noise at time  $t_3$  is the sum of the thermal noise contributed by the reset amplifier, thermal noise from M5, and shot noise from the photodiode current. The shot noise contributed by the photodiode current is small and can be neglected. The noise contributed to  $V_{pd}$  by the reset amplifier is

$$\sigma_{ramp}^2(t_3) = \int_{-\infty}^{\infty} S_{V_{rn}}(f) \left| \frac{v_{pd}}{v_r}(f) \right|^2 df, \quad (12)$$

and

$$\frac{v_{pd}}{v_r}(f) = \frac{g_m}{a + j2\pi fb}, \quad (13)$$

where  $a$  and  $b$  are given in the Appendix. After evaluating the integral, we find

$$\sigma_{ramp}^2(t_3) = \frac{\alpha kT g_m}{ab}. \quad (14)$$

Using the model in Figure 4 and assuming  $v_g$  falls much faster than the time constant of the reset control loop, then the noise power contributed by M5 to  $V_n$  is

$$\sigma_{M5}^2(t_3) = \int_{-\infty}^{\infty} S_{V_{M5}}(f) \left| \frac{v_{pd}}{v_{M5}}(f) \right|^2 df, \quad (15)$$

where  $S_{V_{M5}}(f) = 2kTR_{M5}$ ,  $R_{M5}$  is the channel resistance of M5, and  $\frac{v_{pd}}{v_{M5}}(f)$  is given in the Appendix. The total noise sampled onto the photodiode at  $t_3$  is

$$\sigma_{v_{pd}}^2(t_3) = \sigma_{ramp}^2(t_3) + \sigma_{M5}^2(t_3) + \sigma_{V_n}^2(t_2) \left( \frac{g_o(C_{pd} + C_f)}{C_f a} \right)^2. \quad (16)$$

The final term in equation 16 is the noise sampled on the photodiode at  $t_2$  attenuated by the reset control loop.

By appropriately selecting the gain of the reset amplifier,  $\frac{g_m}{g_o}$ , the overlap capacitance of M1,  $C_f$ , and the bandlimiting capacitance,  $C_{l1}$  and  $C_{l2}$ , pixel reset noise will be much lower than  $\frac{kT}{C}$ . This reduction in reset noise is achieved by turning off M1, bandlimiting the reset amplifier, and by controlling the reset loop via a capacitive voltage divider. Again using values of  $C_{pd}=25.3\text{fF}$ ,  $C_f=0.4\text{fF}$ ,  $C_l=22\text{fF}$ ,  $g_m = 2.37\mu\text{S}$ ,  $g_o = 8.3\text{nS}$ ,  $\alpha = 1$ ,  $i_{pd}(t_3) = 10\text{fA}$ ,  $T = 300\text{K}$ ,  $(t_2 - t_1) = 10\mu\text{s}$ , and  $(t_3 - t_2) = 10\mu\text{s}$ , we find

$$\sigma_{V_{pd}} = 104\mu\text{V}.$$

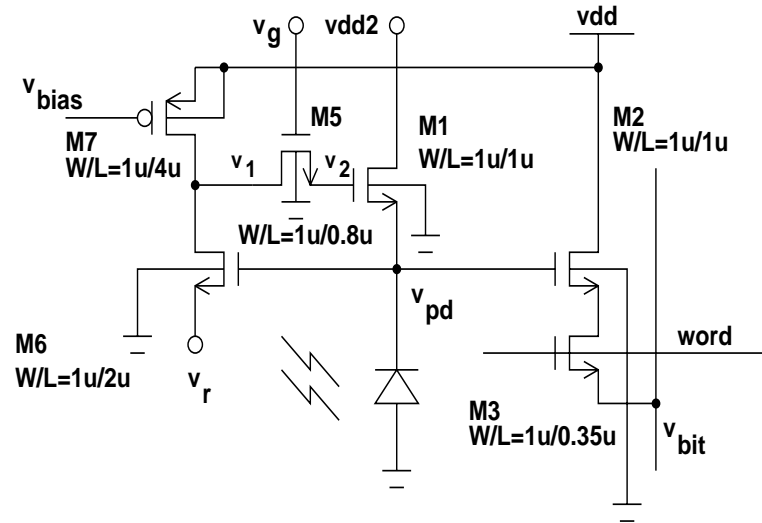
This result corresponds to 16.5 electrons or  $\frac{kT}{15C}$ . If  $g_o$  is reduced to  $0.83\text{nS}$  and  $C_l$  is increased to  $100\text{fF}$ ,  $\sigma_{V_{pd}} = 28\mu\text{V}$ , which corresponds to 4.4 electrons or  $\frac{kT}{210C}$ .

### 3. SIMULATION

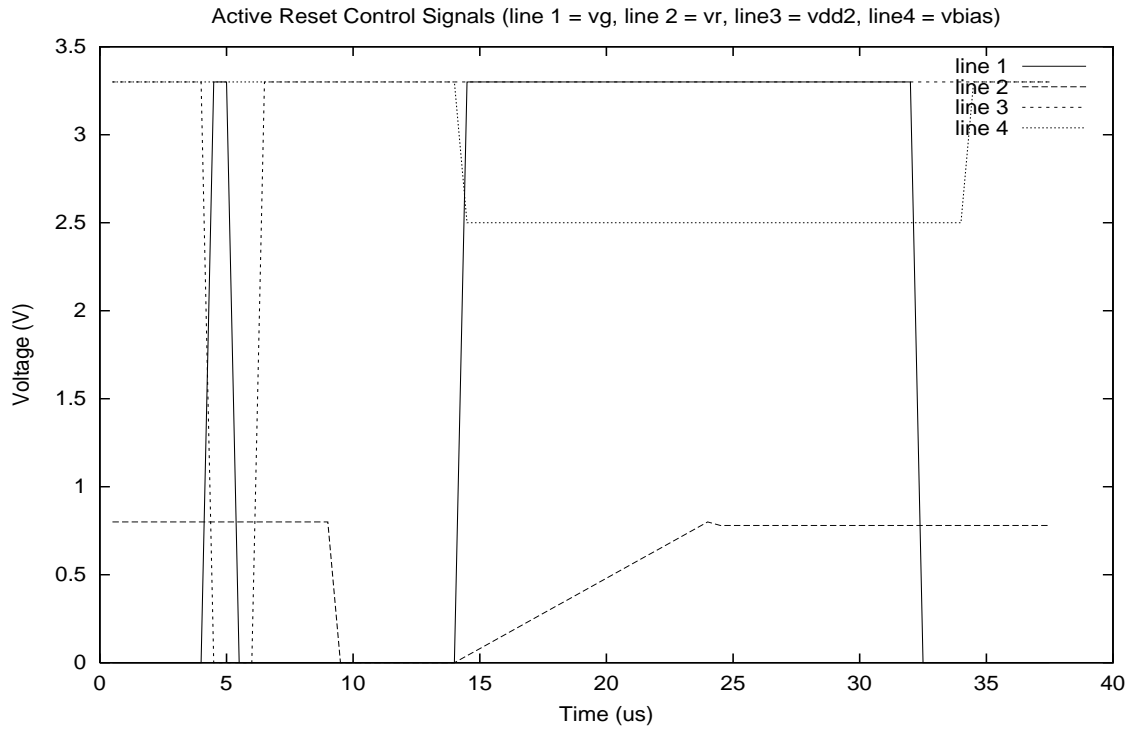
Figure 6 shows a schematic of the 6 transistor  $0.35\mu\text{m}$  active reset pixel used for simulation. We used SPICE to estimate lag and Monte Carlo simulation to estimate noise. Level 49  $0.35\mu\text{m}$  SPICE models were used. The Monte Carlo simulation used 128 iterations.

Figure 6 consists of two sections, the active reset circuit M1, M5, M6, and M7, and the output follower M2 and M3. The active reset feedback amplifier consists of M6 and M7. The positive input of the feedback amplifier is the source terminal of M6 and the negative input is the gate of M6. M1 is initially used to reset the photodiode to ground by setting  $v_{dd2} = 0$  and setting  $v_g = v_{dd}$ . Then M1 is used to complete reset by setting  $v_{dd2} = v_{dd}$  and then ramping  $v_r$  from 0 to 0.8 volts. M6 is used to open the feedback loop after reset is complete. Consistent with theoretical calculations from Section 2, all simulations were performed with  $v_{dd} = 3.3\text{V}$ ,  $i_{pd}(t_7) = 10\text{fA}$ ,  $i_{pd}(t_4) = 2.53\text{pA}$ ,  $(t_2 - t_1) = 10\mu\text{s}$ ,  $(t_3 - t_2) = 10\mu\text{s}$ ,  $\frac{dv_r}{dt}(t_2 - t_1) = 0.08\text{V}/\mu\text{s}$ ,  $\max(v_r) = 0.8\text{V}$ ,  $(t_6 - t_5) = 10\text{ms}$ ,  $C_{pd} = 25.3\text{fF}$ ,  $C_f = 0.4\text{fF}$ ,  $C_l = 22\text{fF}$ ,  $g_m = 2.37\mu\text{S}$ , and  $g_o = 8.3\text{nS}$ , and  $T = 23^\circ\text{C}$ . Figure 7 shows the reset control signals  $v_g$ ,  $v_r$ ,  $v_{dd2}$ , and  $v_{bias}$ . The corresponding SPICE simulation results for  $v_{pd}$ ,  $v_1$ , and  $v_2$  are shown in Figure 8.

SPICE estimates  $\max(\text{lag}) = |(0.22\text{mV})/(-1\text{V})| = 0.022\%$ , and Monte Carlo simulation estimates RMS pixel reset noise  $\sigma_{V_{pd}} = 94\mu\text{V}$ .



**Figure 6.** 6 Transistor Active Reset Pixel Schematic



**Figure 7.** 6 Transistor Active Reset Pixel Control Signals. This figure shows  $v_g$ ,  $v_r$ ,  $v_{dd2}$ , and  $v_{bias}$  as a function of time during pixel reset.

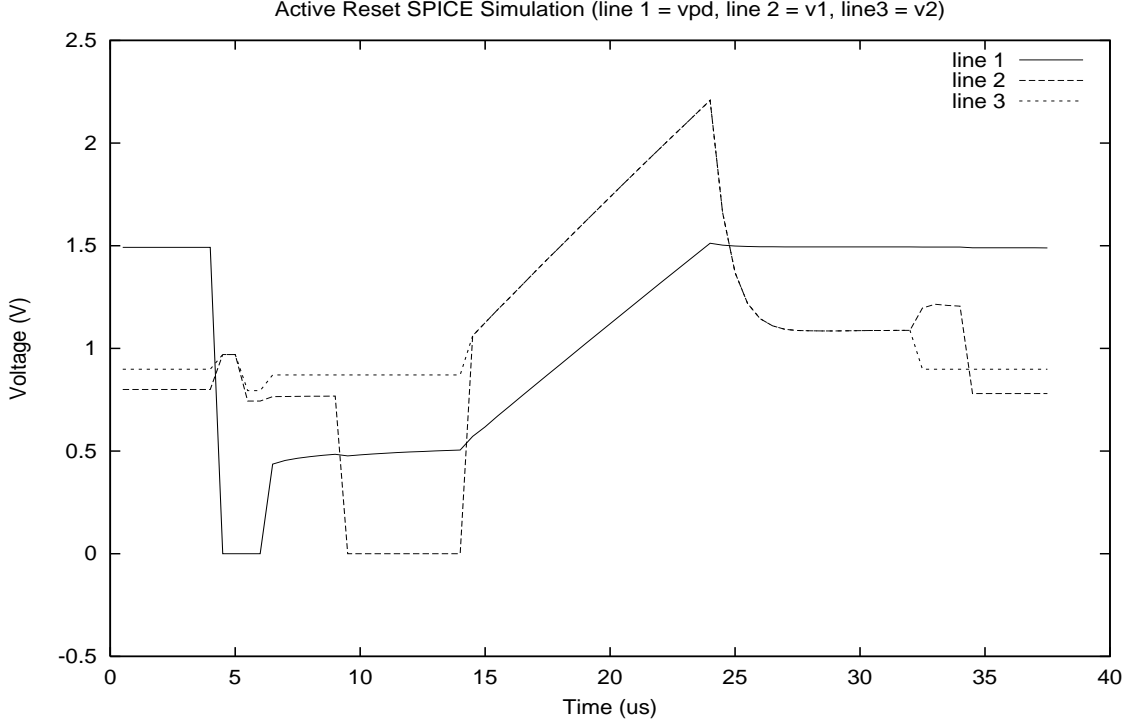


**Figure 8.** 6 Transistor Active Reset Pixel SPICE Simulation. This figure shows  $v_{pd}$ ,  $v_1$ , and  $v_2$  as a function of time during pixel reset.

#### 4. MEASURED RESULTS

In this section, we present lag and noise measurements from a test sensor fabricated in a  $0.35\mu\text{m}$  standard digital CMOS process. Figure 6 shows a schematic of the active reset pixel. The optical and control inputs used for both lag and reset noise measurements were consistent with the values used in simulation (see Section 3).

Lag measurements were performed using a 565nm green LED and an integrating sphere. The LED was placed at the input port of the integrating sphere and the sensor was placed at the output port. The LED was pulsed with a 12.5Hz 50% duty cycle square wave. The pulse amplitude was adjusted to achieve a 1V pixel input-referred signal during a 10ms integration period. Five thousand measurements were used to estimate  $\max(\text{lag})$ . Using this setup, we measured  $v_{bit}(t_5) - v_{bit}(t_7) = 0.17 \pm 0.0034\text{mV}$  and  $v_{bit}(t_4) - v_{bit}(t_7) = -0.85 \pm 0.0001\text{V}^\dagger$ . Using the estimated gain of follower, M2,  $\max(\text{lag}) = |(0.2\text{mV})/(-1\text{V})| = 0.02\%$ .

The optical and electrical setups used to measure noise are described by Fowler *et al.*<sup>8</sup> The analog output of the sensor is amplified using a low noise amplifier (LNA) and digitized using a 16-bit ADC. All noise measurements were taken without illumination. When taking the noise measurements, we first determine the board-level noise, including the LNA noise and the ADC quantization noise. The measured output referred RMS noise voltage was found to be  $28.5(+6.3, -4.5)\mu\text{V}$ . The measured output-referred RMS reset noise voltage of the active reset pixel  $\sigma_{V_{bit}} = 86.3(+19, -14)\mu\text{V}^\S$ . Five thousand samples were used to estimate both board level noise and reset noise of

<sup>†</sup>We estimated the 99% confidence interval using Student's T distribution. This assumes Gaussian noise of unknown power is added to each measurement.

<sup>§</sup>We estimated the 99% confidence interval using  $\sqrt{\frac{(n-1)S^2}{b}} \leq \sigma_{V_{bit}} \leq \sqrt{\frac{(n-1)S^2}{a}}$ , where  $n = 5000$ ,  $S^2 = \frac{1}{n-1} \sum_{i=1}^n (V_{bit}(i) - \overline{V_{bit}})^2$ ,  $a = \chi^2_{n-1, 0.995}$ , and  $b = \chi^2_{n-1, 0.005}$ . This assumes the  $S^2$  statistic is Chi Squared distributed. The 99% confidence interval for the board



the active reset pixel. Using the estimated gain of the follower, M2, and subtracting system noise, the input-referred RMS reset noise voltage  $\sigma_{V_{pd}} = 96\mu\text{V}$ .

## 5. DISCUSSION

Table 1 compares theory, simulation, and measured data for both lag and the reset noise. This comparison is well justified because we used extracted circuit values from the test sensor for both simulation and theoretical calculations, and consistent input and control signals. Theory, simulation, and measured data show close correlation for both lag and reset noise. The measured  $\max(\text{lag})$  value of 0.02% should be invisible in most applications. The  $\frac{kT}{C}$  reset noise of a 25.3fF pixel is 406 $\mu\text{V}$  RMS, and therefore active reset reduces the RMS reset noise by  $\frac{406}{96} = 4.23$ , i.e. the reset noise has been reduced to about  $\frac{kT}{18C}$ .

Lag and Reset Noise Comparison			
	Theory	Simulation	Measurement
$\max(\text{lag})$	0.023%	0.022%	0.02%
$\sigma_{V_{pd}}$	104 $\mu\text{V}$	94 $\mu\text{V}$	96 $\mu\text{V}$

**Table 1.** Active reset lag and reset noise comparison of theory, simulation and measured data.

## 6. CONCLUSIONS

We have shown that active reset can be used to lower reset noise to less than  $\frac{kT}{18C}$  without adding lag. This is nine times less noise power than reported in previous work.<sup>1,2</sup>

Although active reset reduces noise, it requires additional pixel area. In the implementation discussed in Sections 3 and 4, three additional transistors per pixel are required when compared with the standard three transistor APS. In addition, active reset requires more power and a longer reset period than standard APS.

## ACKNOWLEDGEMENTS

We wish to thank Dana How and Hao Min for their helpful comments.

## APPENDIX A. CONSTANTS AND EQUATIONS

$$a = g_o \frac{C_{pd} + C_f}{C_f} + g_m \quad (17)$$

$$b = \frac{C_l C_f + C_{pd} C_f + C_l C_{pd}}{C_f} \quad (18)$$

$$k_1 = v_{pd}(0) - k_2 \quad (19)$$

$$k_2 = \frac{v_r g_m - \frac{C_l + C_f}{C_f} i_{pd} + v_{pd}(0) \frac{C_{pd} + C_f}{C_f} g_o}{a} + \frac{\frac{i_{pd} g_o}{C_f} b}{a^2} - \frac{v_1(0) g_o}{a} \quad (20)$$

$$k_3 = \frac{-i_{pd} g_o}{C_f a} \quad (21)$$

$$\tau = \frac{b}{a} \quad (22)$$

$$k_4 = v_1(0) - k_5 \quad (23)$$

$$k_5 = -\frac{v_1(0) g_m}{a} - v_{pd}(0) \frac{g_m (C_{pd} + C_f)}{C_f a} + \frac{v_r g_m (C_{pd} + C_f)}{C_f a} - \frac{i_{pd} g_m b}{C_f a^2} - \frac{i_{pd}}{a} \quad (24)$$

---

level noise was determined using the same technique.

$$k_6 = \frac{i_d g_m}{C_f a} \quad (25)$$

$$k_7 = \frac{g_o b (i_{pd}(t_5) - i_{pd}(t_7))}{C_f a^2} - \frac{\frac{C_l + C_f}{C_f} (i_{pd}(t_5) - i_{pd}(t_7))}{a} \quad (26)$$

$$k_8 = \frac{-(i_{pd}(t_5) - i_{pd}(t_7))}{C_f} \frac{g_o}{a} \quad (27)$$

$$k_9 = \frac{g_o}{a} \quad (28)$$

$$k_{10} = 1 + \frac{C_{pd}}{C_f} - \frac{g_o b}{C_f a} \quad (29)$$

$$k_{12} = C_l C_f + C_{pd} C_f + C_l C_{pd} \quad (30)$$

$$k_{13} = g_o (C_{pd} + C_f) + g_{m1} C_l + g_{mb1} (C_l + C_f) + g_m C_f \quad (31)$$

$$k_{14} = g_{m1} (g_m + g_o) + g_o g_{mb1} \quad (32)$$

$$\frac{v_{pd}}{v_r}(f) = \frac{j2\pi f C_f + g_{m1}}{(j2\pi f)^2 k_{12} + j2\pi f k_{13} + k_{14}} \quad (33)$$

$$\frac{v_{pd}}{i_d}(f) = \frac{j2\pi f (C_l + C_f) + g_o}{(j2\pi f)^2 k_{12} + j2\pi f k_{13} + k_{14}} \quad (34)$$

$$g_{M5} = \frac{1}{R_{M5}} \quad (35)$$

$$k_{15} = \frac{C_f}{C_f + C_{pd}} \quad (36)$$

$$k_{16} = C_{l2} + C_{ov} + C_{pd} k_{15} \quad (37)$$

$$\frac{v_{pd}}{v_{M5}}(f) = \frac{j2\pi f (C_{l1} + C_{ov}) + g_o}{g_m g_{M5} k_{15} + (j2\pi f) g_{M5} k_{15} + (g_o + j2\pi f (C_{l1} + C_{ov})) (g_{M5} + j2\pi f k_{16})} \quad (38)$$

## REFERENCES

1. B. Pain *et al.*, "Analysis and enhancement of low-light-level performance of photodiode-type CMOS active pixel imagers operated with sub-threshold reset," in *1999 IEEE Workshop on CCDs and AIS*, (Nagano, Japan), June 1999.
2. H. Tian, B. Fowler, and A. El Gamal, "Analysis of Temporal Noise in CMOS APS," in *Proceedings of SPIE*, vol. 3649, (San Jose, CA), January 1999.
3. O. Yadid-Pecht, B. Mansoorian, E. Fossum, and B. Pain, "Optimization of Noise and Responsivity in CMOS Active Pixel Sensor for Detection of Ultra Low Light Levels," in *Proceedings of SPIE*, vol. 3019, (San Jose, CA), January 1997.
4. S. Mendis *et al.*, "Progress in CMOS Active Pixel Image Sensors," in *Proceedings of SPIE*, pp. 19–29, (San Jose, CA), February 1994.
5. A. El Gamal, B. Fowler, and H. Min, "Modeling and Estimation of FPN Components in CMOS Image Sensors," in *Proceedings of SPIE*, vol. 3301, (San Jose, CA), January 1998.
6. T. Nobusada *et al.*, "Frame Interline CCD Sensor for HDTV Camera," in *ISSCC Digest of Technical Papers*, (San Francisco, CA, USA), February 1989.
7. A. Van der Ziel, *Noise in Solid State Devices*, Wiley, New York, 1986.
8. B. Fowler, A. El Gamal, and D. Yang, "A Method for Estimating Quantum Efficiency for CMOS Image Sensors," in *Proceedings of SPIE*, vol. 3301, (San Jose, CA), January 1998.